Theory of alloys. III. Embedded-cluster calculations of electronic spectra for a one-dimensional ternary alloy

Yu-Tang Shen and Charles W. Myles
Department of Physics and Engineering Physics, Texas Tech University, Lubbock, Texas 79409
(Received 13 July 1983; revised manuscript received 15 March 1984)

The embedded-cluster method is modified to treat electronic spectra in ternary alloys and is applied to the calculation of the electronic density of states for the one-dimensional, one-state-per-atom, ternary alloy $A_xB_{1-x}C$ in the nearest-neighbor tight-binding approximation. As a test of this method, the spectra for some representative cases of alloys in the "persistence" and "amalgamation" regimes are presented and compared with "exact" spectra for the same cases obtained for 10 000-atom random chains by the use of the negative-eigenvalue theorem. For a cluster containing eight unit cells embedded in a coherent-potential-approximation effective medium, the embedded-cluster method reproduces all of the major features of the exact spectra for all alloy compositions and over wide range of atomic energies of the alloy constituents.

I. INTRODUCTION

Recently, there have been a number of experimental and theoretical investigations of the electronic properties of the ternary semiconducting alloys.[1–9] These studies have been stimulated in part by the increasing technological importance of these materials for use in such diverse device applications as light-emitting diodes, infrared detectors, and solid-state lasers. However, these materials are also interesting in their own right as prototypes for the study of the basic physics and chemistry of disordered electronic systems. The first comprehensive theory of the ternary semiconducting alloys which can be used to make predictions of their electronic properties over the entire range of alloy compositions was formulated by Chen and Sher.[7] Ehrenreich and Hass have also recently developed such a theory.[8] These workers have treated the effects of alloy disorder on the electronic band structure in these materials by the use of the coherent-potential approximation (CPA). While such a theory is sufficient for treating the dependence of global electronic properties on the alloy composition, it is well known[10] that the CPA neglects all short-range order due to local clustering of alloy constituents. It will thus be expected to be inadequate to explain experiments which measure such short-range-order effects. Measurements which fall into this category are those which are sensitive probes of the local electronic state density, as for example, photoluminescence from impurities.[1,6] A theory which includes such short-range-order effects and which is also computationally tractable for application to real semiconductor alloys does not, at present, exist.

Gonis and Garland[11] laid the foundation for such a theory with their general treatment of clusters of atoms embedded in effective media. Using this general theory as a basis, Myles and Dow[12,13] developed the embedded-cluster method, in which the effective medium used is the one appropriate for the single-site CPA and in which an average of the state densities of all possible configurations of alloy constituents in a cluster embedded in an appropriate effective medium is used to approximate the alloy-state density. These same workers also tested this method in application to the calculation of the frequency distribution spectra of lattice vibrations in model one-dimensional binary[13] and ternary[12,14] alloys. For these model systems, this technique has successfully and easily reproduced the exact numerical spectra obtained for several-thousand-atom random chains by the use of the negative-eigenvalue theorem.[15,16]

The first application of the embedded-cluster method to realistic three-dimensional models of alloys has very recently been made to metallic binary alloys by Gonis *et al.*[17] Using a Korringa-Kohn-Rostoker[18] (KKR) Hamiltonian as input, these workers have embedded clusters of alloy constituents in a CPA effective medium and have, in this manner, successfully treated the effects of clustering on the electronic density of states in $Ag_{1-x}Pd_x$ alloys. They have furthermore shown that this method may be used to systematically investigate charge transfer and short-range-order effects in such alloys.

The purpose of the present paper is to modify the embedded-cluster method for application to electronic spectra in ternary alloys and to further test this method by applying it to the calculation of the electronic spectra for the one-dimensional, one-state-per-atom, nearest-neighbor, tight-binding model ternary alloy. This model is clearly much too crude to enable us to obtain any quantitative understanding of electronic spectra in semiconductor alloys. Nevertheless, it can be used to obtain a qualitative understanding of how clustering and short-range order can affect such spectra without the complications of a realistic, three-dimensional, multiband, multineighbor model. The initial treatment of such a simple model also has the advantage of enabling us to develop a calculational technique and to test it on a system which is simple enough that the physics of clustering and short-range order is not obscured by other effects. We compare the results of our calculations on this model to "exact" spectra for 10 000-atom random chains obtained for the same cases by the use of the negative-eigenvalue

 ©1984 The American Physical Society

theorem.[15,16] We find that the embedded-cluster method shows an advantage over even these exact calculations and is complementary to them in that it can easily be used to identify and label peaks in the spectra which are due to persistent[19] electronic states associated with small clusters of atoms containing particular configurations of alloy constituents.[12–14,16] It is hoped that the present calculations will be useful because they may be used to obtain a qualitative understanding of the effects of clustering and short-range order on electronic spectra in ternary alloys. A more quantitative understanding of these effects must await more realistic calculations, which we are presently pursuing.[20]

The present paper is the third of a series. The first two papers in this series may be found in Ref. 13 (referred to henceforth as I) and Ref. 14 (referred to henceforth as II), respectively.

The remainder of this paper is organized as follows. In Sec. II the notation to be used and the basic model to be considered are discussed, and the electronic properties of a perfect diatomic chain are briefly reviewed. Section III contains a brief discussion of the coherent potential approximation[10,19,21–24] as applied to electronic spectra in ternary alloys. The embedded-cluster method for electronic spectra in ternary alloys is discussed in Sec. IV, and Sec. V presents results of embedded-cluster calculations of the electronic spectra of several model one-dimensional ternary alloys and comparisons with exact results obtained for 10 000-atom random chains by the use of the negative-eigenvalue theorem. This comparison shows that, using an eight unit-cell cluster embedded in a coherent-potential-approximation medium, the embedded-cluster method reproduces all of the major features of the exact spectra for all alloy compositions and over a wide range of atomic energies of the constituents. Finally, Sec. VI contains a brief discussion of the results and some conclusions. The reader not interested in the calculational details may proceed directly to Sec. V.

II. MODEL AND NOTATION

A. Hamiltonian and Green's function for the alloy

In this paper we consider a one-dimensional model ternary alloy $A_xB_{1-x}C$ in the one-state-per-atom, nearest-neighbor tight-binding approximation. Although all of the explicit calculations are done for this simple model, much of the formalism described below is applicable in a straightforward but tedious manner to three dimensions and to alloy systems with more realistic electronic structure.

The alloy one-electron Hamiltonian in the tight-binding approximation is

$$H=\sum_{n,\alpha}|n,\alpha\rangle\epsilon_{n\alpha}\langle n,\alpha|+\sum_{\substack{n,n',\\ \alpha,\alpha'}}|n,\alpha\rangle t_{nn'}^{\alpha\alpha'}\langle n',\alpha'|\ , \tag{1a}$$

where $|n,\alpha\rangle$ is the atomiclike orbital of the αth atom ($\alpha=1$ or 2) in the nth unit cell and $\alpha=1$ ($\alpha=2$) refers to the sublattice with A or B (C) atoms. Here we consider diagonal disorder only; thus the on-site matrix element $\epsilon_{n\alpha}$ has the form

$$\epsilon_{n\alpha}=\delta_{\alpha,1}\epsilon_{n1}+\delta_{\alpha,2}\epsilon_C\ , \tag{1b}$$

where ϵ_{n1} is a random variable taking on the values ϵ_A and ϵ_B with probabilities x and $1-x$, respectively, and ϵ_A, ϵ_B, and ϵ_C are the atomiclike energies of the A, B, and C atoms. Furthermore, the nearest-neighbor transfer-matrix element is

$$t_{nn'}^{\alpha\alpha'}=t[\delta_{\alpha,1}\delta_{\alpha',2}(\delta_{n',n-1}+\delta_{n,n'})+\delta_{\alpha,2}\delta_{\alpha',1}(\delta_{n',n+1}+\delta_{n,n'})]\ , \tag{1c}$$

where the nearest-neighbor interaction energy t is assumed to be the same for the two possible pairs AC and BC and to be independent of x.

The alloy Green's-function matrix is defined as

$$G=(E-H+i0)^{-1} \tag{2}$$

where E is an energy and $i0$ is a positive imaginary infinitesimal. One of the primary quantities of interest in the present paper is the configuration-averaged alloy density of states, which is defined in the usual manner[10] as

$$D(E)=-\frac{1}{\pi N}\mathrm{Im}\{\mathrm{Tr}\langle\langle G\rangle\rangle\}\ , \tag{3}$$

where the trace runs over all unit cells in the crystal, N is the total number of unit cells, and the double angular brackets here and henceforth denote an average over all alloy configurations.

B. Solutions for the ordered diatomic crystal

In the limit where the atoms A and B become identical, the "alloy" becomes the ordered diatomic lattice BC, atom B occupies sublattice 1 and ϵ_{n1} is always equal to ϵ_B. For this case in one dimension, the energy bands, the corresponding eigenfunctions, the real-space matrix elements of the Green's function, and the density of states can all easily be obtained in closed form. The energy bands are

$$E_j(k)=\epsilon_+\pm[\epsilon_-^2+4t^2\cos^2(ka/2)]^{1/2}\ , \tag{4}$$

where k is a wave vector in the first Brillouin zone, a is the lattice constant (the nearest-neighbor distance is $a/2$), $\epsilon_\pm=(\epsilon_C\pm\epsilon_B)/2$, and for $j=v$ (valence band) the minus sign applies, while for $j=c$ (conduction band) the plus sign applies. The orthonormalized eigenfunctions corresponding to these eigenvalues are given in Appendix A. As is also discussed in Appendix A, the Green's-function matrix elements for this case can, after much manipulation, be brought in the form

$$G_{\alpha\alpha}^0(n,n',E)=[(E-\epsilon_C)\delta_{\alpha,1}+(E-\epsilon_B)\delta_{\alpha,2}]\times A(n,n',E)\ , \tag{5a}$$

and

$$G^0_{12}(n,n',E)=[G^0_{21}(n',n,E)]^* \\ =t[A(n,n',E)+A(n-1,n',E)] , \quad (5b)$$

where we have used the shorthand notation $\langle n,\alpha \mid G^0(E) \mid n',\beta\rangle \equiv G^0_{\alpha\beta}(n,n',E)$ for the real-space Green's-function matrix elements and the superscript denotes that this function is for the ordered diatomic chain. As is discussed in Appendix A, the function $A(n,n',E)$ can, by using standard mathematical techniques, be expressed in closed form as

$$A(n,n',E)=\pm\frac{\left[\frac{(E-\epsilon_B)(E-\epsilon_C)}{2t^2}-1\mp\frac{(E-\epsilon_B)^{1/2}(E-\epsilon_C)^{1/2}(E-E_v)^{1/2}(E-E_c)^{1/2}}{2t^2}\right]^{|n-n'|}}{(E-\epsilon_C)^{1/2}(E-\epsilon_B)^{1/2}(E-E_v)^{1/2}(E-E_c)^{1/2}} , \quad (5c)$$

where the upper (lower) signs apply for $(E-E_v)(E-E_c)>0(<0)$ and E_v (E_c) means $E_v(k=0)$ [$E_c(k=0)$]. In Eq. (5c) and in what follows, the square roots must be evaluated in their complex sense; that is, if the argument of the square root is positive, the positive square root is taken, while if the argument is negative, the positive imaginary root is taken. The density of electronic states for the perfect chain can be evaluated by combining Eqs. (3) and (5). The result is

$$D^0(E)=-\frac{1}{\pi}\mathrm{Im}\left[\frac{|2E-\epsilon_B-\epsilon_C|}{(E-\epsilon_B)^{1/2}(E-\epsilon_C)^{1/2}(E-E_v)^{1/2}(E-E_c)^{1/2}}\right] . \quad (6)$$

Several features which are present in this function tend to persist to some extent in the alloy electronic spectra discussed below. In particular, $D^0(E)$ is symmetric about the center of the band gap and is normalized to $\int_{-\infty}^{\infty} dE\, D^0(E)=2$, the bottom of the valence band occurs at $E_v=\epsilon_+-(\epsilon_-^2+4t^2)^{1/2}$, the top of the valence band occurs at ϵ_B, the bottom of the conduction band occurs at ϵ_C, the top of the conduction band occurs at $E_c=\epsilon_++(\epsilon_-^2+4t^2)^{1/2}$, and the band gap is equal to $\epsilon_C-\epsilon_B$. (We have implicitly assumed $\epsilon_C>\epsilon_B$ in this discussion.) It is often possible to, at least grossly, view the spectra for the alloy $A_xB_{1-x}C$ as some combination of the spectrum of the pure BC chain [Eq. (6)] with the pure AC chain spectrum [Eq. (6) with ϵ_B replaced by ϵ_A], superimposed upon the "impurity" spectra of A defects in the BC chain or vice versa. Thus it is useful to keep the perfect-chain spectrum in mind when discussing the alloy spectra.

III. COHERENT-POTENTIAL APPROXIMATION

Although theoretical investigations of substitutionally disordered alloys began a number of years ago,[25] no theory has as yet been more than partially successful in its prediction of alloy electronic spectra. A coherent potential theory of ternary alloys was first discussed by Taylor[22] in 1973 and independently by Sen and Hartmann in 1974.[24] Both of these investigations were of the vibrational spectra of such alloys. Recently, both Chen and Sher[7] and Ehrenreich and Hass[8] have developed CPA theories of the electronic energy bands of real ternary semiconducting alloys.

Since the best single-cell effective-medium theory is the coherent-potential approximation[10] and since we have found that the CPA is also the best effective medium to use as a cluster boundary condition in implementing the embedded-cluster method discussed below, it is worthwhile to briefly review this theory for electronic spectra in ternary alloys. The following discussion is a generalization of the theory of Sen and Hartmann[24] to electronic spectra and closely parallels the discussion of phonon spectra in their paper.

One approach to the theory of the electronic properties of the alloy $A_xB_{1-x}C$ is to begin by considering this alloy as a BC crystal containing a large number of randomly distributed A impurities with concentration x. The alloy Green's function for a specific configuration and for A impurities occupying the $\alpha=1$ sublattice then satisfies the Dyson equation

$$G=G^0+G^0VG , \quad (7)$$

where G^0 is the perfect BC crystal Green's function and the defect matrix V has the form

$$V=H-H_0 \quad (8a)$$

or

$$V=\sum_n v_n=\sum_n |n,1\rangle(\epsilon_{n1}-\epsilon_B)\langle n,1| . \quad (8b)$$

Here H_0 is the perfect crystal Hamiltonian and Eq. (8b) follows in the present model from the assumption of diagonal disorder. An exact solution to Eq. (7) is not possible for arbitrary composition x. Furthermore, for this general case, the distinction between "defect" and "host" atoms becomes arbitrary and any correct theory should predict results which are independent of this choice. Thus, in what follows, we arbitrarily denote the defect atom as an A atom, the host atom as a B atom and label the disordered sublattice with the index $\alpha=1$.

A common approximation to the solution of Eq. (7) is to replace the random alloy by a translationally invariant effective medium. The effective-medium Green's function is defined as the configuration average of the alloy Green's function G,

$$g=\langle\langle G\rangle\rangle . \quad (9)$$

In the single-cell CPA this function satisfies the equation

$$g = G^0 + G^0 \Sigma g = (E - H_0 - \Sigma + i0)^{-1} , \tag{10}$$

where Σ is the (to be determined) self-energy matrix. In the single-cell CPA the Green's function g is determined self-consistently by requiring that (i) the effective medium's quasiparticles scatter the minimum amount; that is, that the single-cell effective-medium transition matrix vanishes when averaged over all possible alloy configurations and that (ii) the self-energy assumes the form

$$\Sigma(E) = \sum_n \sigma_n = \sum_n | n,1 > \epsilon_B \tilde{\sigma}(E) < n,1 | , \tag{11}$$

where $\tilde{\sigma}(E)$ is the single-cell self-energy. Requirement (ii) physically means that the effective medium is translationally invariant and that all unit cells in the medium are equivalent. Sen and Hartmann[24] have shown that the 2×2 matrix σ_n is nonzero only on the defect ($\alpha = 1$) sublattice for cubic lattices in one, two, and three dimensions.

In order to carry out the CPA, Eqs. (7) and (10) are combined to obtain an expression for G in terms of the effective-medium Green's function g:

$$G = g + g(V - \Sigma)G = g + gTg , \tag{12}$$

where we have defined an effective-medium transition matrix T as

$$T = (V - \Sigma)[I - g(V - \Sigma)]^{-1} . \tag{13a}$$

Here I is the unit matrix. In the single-cell CPA one assumes that T is the sum over the unit cell index of single-cell transition matrices t_n which have the form

$$t_n = (v_n - \sigma_n)[1 - g_n(v_n - \sigma_n)]^{-1} , \tag{13b}$$

where 1 means the 2×2 unit matrix and g_n is the Green's function

$$\langle n | g | n \rangle = \langle n = 0 | g | n = 0 \rangle = \sum_{\alpha,\beta} \langle n | n,\alpha \rangle g_{\alpha\beta} \langle n,\beta | n \rangle .$$

Combining Eqs. (12) and (13) and requiring that the effective-medium Green's function satisfy Eq. (9) leads to the self-consistency requirement that the configuration average of t_n vanish [which is just requirement (i) above]. This results, after some manipulation, in the 2×2 matrix equation

$$\sigma_n - xv + \sigma_n g_n (\sigma_n - v) = 0 . \tag{14a}$$

where v is a 2×2 matrix defined by

$$v_{\alpha\beta} = (\epsilon_A - \epsilon_B)\delta_{\alpha,\beta}\delta_{\alpha,1} . \tag{14b}$$

Use of Eqs. (14a), (14b), and (11) finally yields a scalar equation for the single-cell self-energy $\tilde{\sigma}(E)$:

$$\epsilon_B \tilde{\sigma}(E) - x(\epsilon_A - \epsilon_B) + \epsilon_B \tilde{\sigma}(E)[\epsilon_B \tilde{\sigma}(E) - (\epsilon_A - \epsilon_B)] g_{11}(E) = 0 , \tag{15}$$

where $g_{11}(E) = \langle n,1 | g | n,1 \rangle$.

One can easily obtain closed form expressions for the CPA Green's functions in the site representation by combining Eqs. (10) and (5). Considerable manipulation leads to the expression

$$g_{\alpha\beta}(n,n',E) = B_{\alpha\beta}(E) G^0_{\alpha\beta}(n,n',Z) , \tag{16a}$$

where

$$B_{\alpha\beta}(E) = (E - \epsilon_C)(Z - \epsilon_C)^{-1}\delta_{\alpha,\beta}\delta_{\alpha,1} + (Z - \epsilon_C)(E - \epsilon_C)^{-1}\delta_{\alpha,\beta}\delta_{\alpha,2} + \delta_{\alpha,1}\delta_{\beta,2} + \delta_{\beta,1}\delta_{\alpha,2} \tag{16b}$$

and where the complex variable Z is expressed in terms of $\tilde{\sigma}(E)$ as

$$Z = \epsilon_+ + [(E - \epsilon_+)^2 - (E - \epsilon_C)\epsilon_B \tilde{\sigma}(E)]^{1/2} . \tag{16c}$$

Upon setting $n = n'$ in Eq. (16a) and combining that equation with Eqs. (16c), (5), and (15), a cubic algebraic equation for the self-energy $\tilde{\sigma}(E)$ of the form

$$a_3 \tilde{\sigma}^3 + a_2 \tilde{\sigma}^2 + a_1 \tilde{\sigma} + a_0 = 0 \tag{17}$$

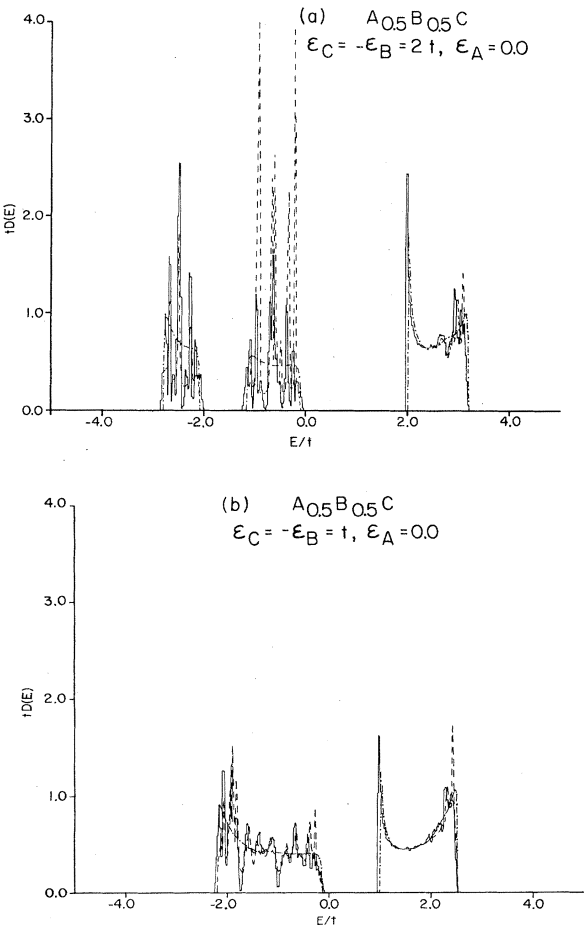

FIG. 1. Density of states $D(E)$ for the one-dimensional ternary alloy $A_{0.5}B_{0.5}C$ with $\epsilon_C = -\epsilon_B$ and $\epsilon_A = 0.0$, obtained by the negative-eigenvalue-theorem method for a 10 000-atom random chain (histograms), by the coherent-potential approximation (dotted-dashed curves), and by embedded-cluster method with $N_c = 8$ (dashed curves) for the cases (a) $\epsilon_C = 2t$ and (b) $\epsilon_C = t$. These two cases illustrate typical spectra for an alloy in the persistence and the amalgamation limits, respectively.

is obtained, where a_0, a_1, a_2, and a_3 are functions of ϵ_A, ϵ_B, ϵ_C, x, E, and t. Explicit expressions for these quantities are shown in Appendix B.

The CPA density of states has the form

$$D_{\mathrm{CPA}}(E)=-\frac{1}{\pi}\mathrm{Im}[g_{11}(n,n,E)+g_{22}(n,n,E)] . \quad (18)$$

This CPA result is illustrated for $x=0.5$ in Fig. 1 (dotted-dashed curves) for two different ternary alloys. Figure 1(a) shows the case of an alloy in the "persistence"[19] regime ($x=0.5$, $\epsilon_C=-\epsilon_B=2t$, $\epsilon_A=0$), where three bands (two valence bands and one conduction band) are distinguishable. On the other hand, Fig. 1(b) shows the case of a typical "amalgamation"[19] type alloy, ($x=0.5$, $\epsilon_C=-\epsilon_B=t$, $\epsilon_A=0$), where two bands (one valence band and one conduction band) are present. For comparison, the negative-eigenvalue theorem results for a 10 000-atom chain (histogram) and the embedded-cluster method results, obtained using an eight-unit-cell cluster (dashed curves) are also shown in these figures. The evident failure of the CPA to reproduce the fine structure of the exact spectra is due to the well-known fact that it neglects the short-range order which is responsible for this structure. (The CPA was not designed to reproduce such spectra, but to provide a self-consistent interpolation between the $x=0$ and 1 limits.[10]) The embedded-cluster method, by contrast, accurately mimics all of the major features of the exact spectra.

IV. EMBEDDED-CLUSTER THEORY

The present theory is very similar to the treatment of vibrational spectra in binary and ternary alloys discussed in I and II, is similar in spirit to the general treatment of clusters in effective media done by Gonis and Garland,[11] and is also similar to the recent treatment of clustering in metallic alloys by Gonis, Butler, and Stocks.[17] The starting point for our theory is an effective-medium representation for the random alloy $A_xB_{1-x}C$; in the usual case we take this to be the CPA medium.[26] The medium is thus characterized by a self-energy Σ and has a Green's function of the form given by Eq. (10). A cluster containing N_c unit cells [with xN_c of them containing AC and $(1-x)N_c$ of them containing BC] in a particular configuration is embedded in this medium. The cluster Green's function for this configuration has the general form given by Eq. (2) for sites within the cluster. Our approximation for the alloy Green's function is that it be of this form inside the cluster and take the form of the effective-medium Green's function, Eq. (10), outside the cluster. We then define an effective scattering potential, which has the form

$$V^*=V-\Sigma=H-H_0-\Sigma \quad (19)$$

inside the cluster and which vanishes outside the cluster. Using this potential, the cluster Green's function, Eq. (2), may be related to the effective-medium Green's function, Eq. (10), by the Dyson equation

$$G=g+gV^*G=(1-gV^*)^{-1}g . \quad (20)$$

This equation is solved numerically for atoms within the cluster (since $G=g$ outside the cluster).

The electronic density of states in this approximation is obtained by first calculating the average of G over all k configurations of the N_c cell cluster[27]

$$\langle\langle G\rangle\rangle=k^{-1}\sum_{j=1}^{k}(G)_j , \quad (21a)$$

where $(G)_j$ is the function given by Eq. (2) for the jth configuration. From $\langle\langle G\rangle\rangle$ one calculates the cluster density of states, which is given by

$$D(E;N_c)=-\frac{1}{N_c\pi}\sum_{n=1}^{N_c}\mathrm{Im}[\langle\langle G_{11}(n,n,E)\rangle\rangle + \langle\langle G_{22}(n,n,E)\rangle\rangle] . \quad (21b)$$

The primary approximation of our theory is that the density of states obtained by this procedure is the configuration averaged density of states for the random alloy.

Other varieties of state density are as easily calculated using our theory as is the total density of states. For example, here we consider the total density of states for a specific cluster configuration

$$d(E;N_c)=-\frac{1}{\pi N_c}\mathrm{Im}[\mathrm{Tr}_c(G)] , \quad (22a)$$

and the local density of states for the nth unit cell within this configuration

$$\Delta_n(E;N_c)=-\frac{1}{\pi}\mathrm{Im}\left[\sum_{\alpha}\langle n,\alpha\,|\,G\,|\,n,\alpha\rangle\right] . \quad (22b)$$

Here Tr_c means a trace over all sites of the cluster. The quantity Δ_n should be independent of n if the cluster size is sufficiently large. In practice, we select a central cell to minimize boundary effects.

Following I and II, in the results presented below we have included only configurations of a given cluster size whose composition is equal to the average composition x. As is discussed in II, the resulting small increase in accuracy which would be obtained by keeping the atypical configuration whose compositions differ from x would not be worth the tremendous increase required in the number of configurations computed.[28,29]

V. NUMERICAL RESULTS FOR THE DENSITY OF STATES; COMPARISON OF EMBEDDED CLUSTER AND EXACT CALCULATIONS

We have calculated the total density of states for a number of different one-dimensional ternary alloys using the embedded-cluster method, Eqs. (19)—(21). For comparison, we have also calculated the exact spectra for the same cases for 10 000-atom random chains using the negative-eigenvalue theorem.

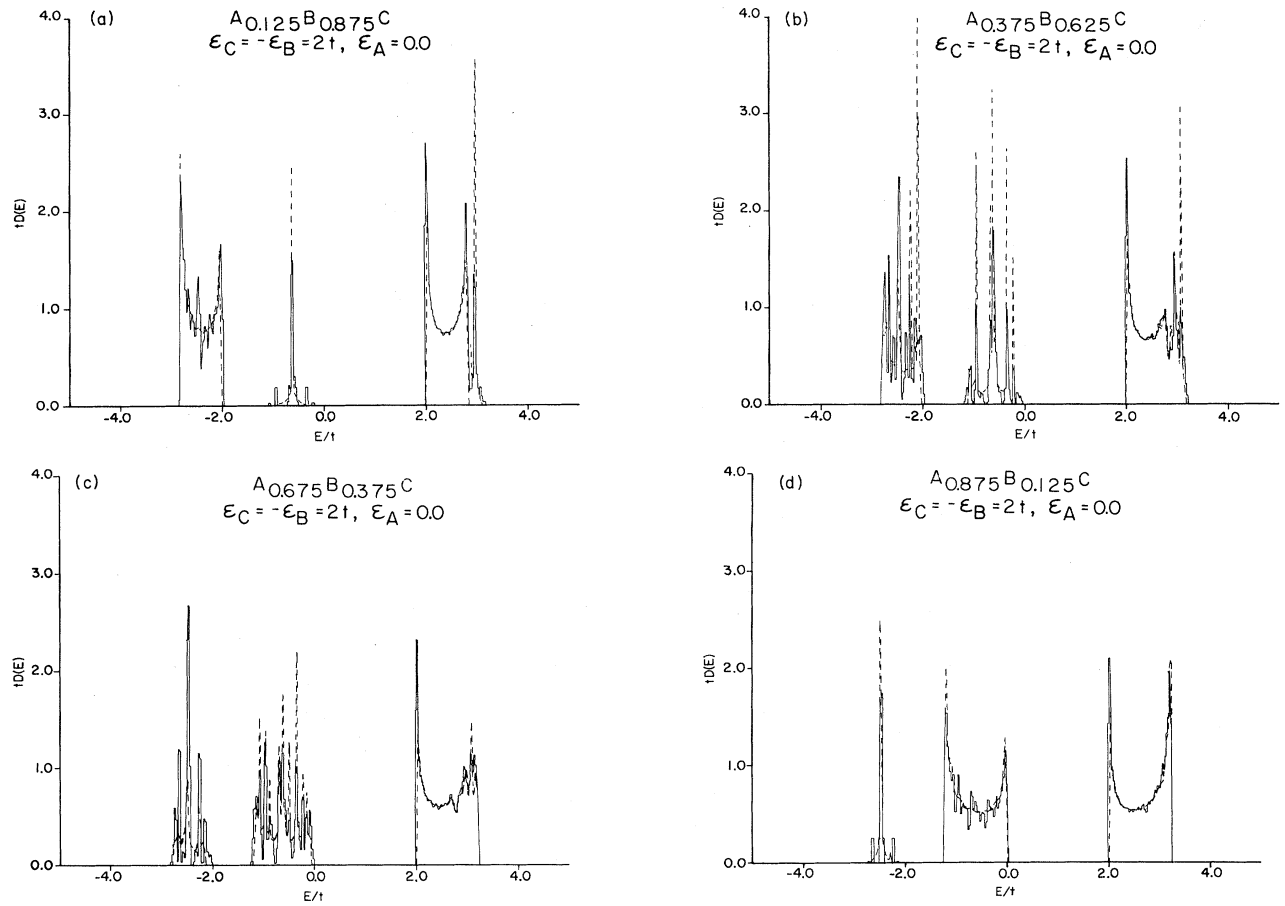

FIG. 2. Density of states $D(E)$ for the one-dimensional ternary alloy $A_xB_{1-x}C$ for the case $\epsilon_C = -\epsilon_B = 2t$ and $\epsilon_A = 0.0$ obtained by the embedded-cluster method with an $N_c = 8$ unit cell cluster (dashed curves) and by the negative-eigenvalue theorem for a 10000-atom random chain (histograms) for the composition x equal to (a) 0.125, (b) 0.375, (c) 0.625, and (d) 0.875.

A. Dependence of composition x; alloys in the persistence and amalgamation limits

The composition dependences of the spectra for two different one-dimensional alloys are displayed in Figs. 2 and 3 for the compositions $x = 0.125$, 0.375, 0.625, and 0.875. The spectra shown in Fig. 2 are for an alloy in the persistence limit ($\epsilon_C = -\epsilon_B = 2t$, $\epsilon_A = 0$), where the bands of the constituents AC and BC persist in the alloy. On the other hand, the spectra shown in Fig. 3 are for an alloy in the amalgamation limit ($\epsilon_C = -\epsilon_B = t$, $\epsilon_A = 0$), where the alloy spectra are characteristic of neither AC nor BC, but instead are a mixture which is characteristic of the alloy itself. These two cases have been chosen for illustration in order to display, at the same time, the dependence of the spectra on the constituent atomic energy differences. The spectra of these same two alloys for composition $x = 0.5$ are shown in Fig. 1.

The exact calculations are shown in Figs. 1–3 as histograms, while the embedded-cluster-method results are shown as dashed curves. All of the embedded-cluster-method results are for a cluster size of $N_c = 8$ unit cells. As may be seen from an inspection of these figures, the embedded-cluster-method calculations reproduce all of the principal features of the exact spectra. The two unsatisfactory features of these results are essentially the same as those noted for phonon spectra in II. These are that (1) due to our choice of the CPA medium at the boundary, the band edges and gaps are sometimes incorrectly predicted by the theory (the embedded-cluster theory will produce no states where the CPA has a gap) and (2) due to our choice of cluster size and the fact that we have included only clusters with the average composition x, the peak intensities are sometimes in slight disagreement with those obtained in the exact calculations. These difficulties could, in principle, be overcome by the use of one of the many cluster CPA theories,[10,30,31] which include the cluster self-consistently and/or by using larger clusters and including the less probable configurations in our calculations.[28,29] However, as is discussed in more detail in II, each of these possibilities would greatly increase the computational complexity of the method and decrease its potential practicality for application to real alloys.

We have also calculated the electronic density of states for crude one-dimensional models of a number of technologically important alloys. For purposes of illustration here we only show results for $GaAs_{1-x}P_x$ and $Hg_{1-x}Cd_xTe$ at $x = 0.5$.[32] These two particular cases

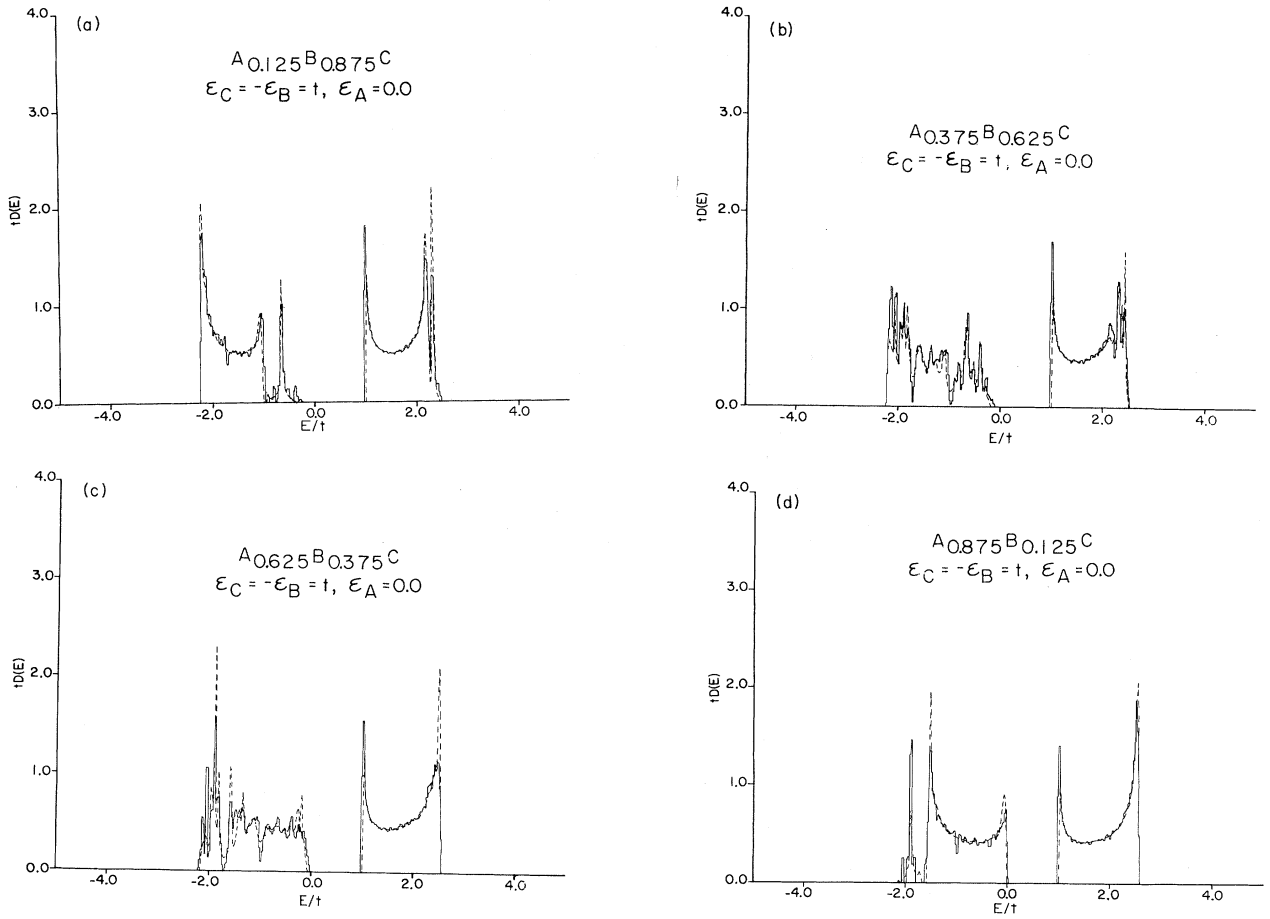

FIG. 3. Density of states $D(E)$ for the one-dimensional ternary alloy $A_xB_{1-x}C$ for the case $\epsilon_C = -\epsilon_B = t$ and $\epsilon_A = 0.0$ obtained by the embedded-cluster method with an $N_c = 8$ unit-cell cluster (dashed curves) and by the negative-eigenvalue theorem for a 10000-atom random chain (histograms) for the composition x equal to (a) 0.125, (b) 0.375, (c) 0.625, and (d) 0.875.

were chosen because they represent a wide variation in the atomic energy differences of the alloy constituents. The tight-binding parameters for these models of the alloy $A_xB_{1-x}C$ were chosen in the manner discussed in Ref. 33 using the band gaps of Refs. 34 and 35. The spectrum for "$GaAs_{0.5}P_{0.5}$" ($\epsilon_C = 2.35t$, $\epsilon_B = 0.80t$, $\epsilon_A = 0.0$) is shown in Fig. 4(a), while that for "$Hg_{0.5}Cd_{0.5}Te$" ($\epsilon_C = 0.0$, $\epsilon_B = -0.28t$, $\epsilon_A = 1.59t$) is shown in Fig. 4(b). The exact calculations are again shown as histograms, with the embedded-cluster-method results, obtained with $N_c = 8$ unit cells, shown as dashed curves.

B. Discussion of the features of individual spectra

The individual spectra displayed in Figs. 1–4 are rich in detail which would be missed by an effective-medium theory such as the CPA. Furthermore, they exhibit a large amount of complex structure which is due to clustering effects.

The major spectral peak energies are independent of alloy composition on the scale of the figures. Each peak can be shown to correspond to a characteristic energy of an "island" of several atoms within the long chain.[15,16] Because the probability of a specific island occurring varies significantly as the alloy composition is altered, the height of an island's spectral density peaks will vary in a corresponding way, even though the characteristic energies of that island do not depend on x. The specific islands or configurations of atoms which are responsible for the various peaks in the spectra would be difficult to identify using the negative-eigenvalue-theorem method.[15,16] On the other hand, such identifications are easily made using the embedded-cluster method, since it requires the calculation of the spectra for every possible cluster configuration. An example where these identifications are made is shown in Fig. 4(a) for $GaAs_{0.5}P_{0.5}$. The numbers labeling the peaks in that figure correspond to the cluster configurations shown in Table I. Since the peaks merely change in intensity, but do not significantly shift as x is changed, all of the principal peaks in the spectra for other compositions could be identified using this table.

A detailed examination of the spectra in Figs. 1–4 shows several interesting features which are worth a few comments. The spectra for the typical alloy in the persistence limit, Figs. 1(a) and 2, and the spectra for the typical alloy in the amalgamation limit, Figs. 1(b) and 3, share the characteristic that the majority of the clustering effects occur in the host-valence or impurity-valence

TABLE I. Major clusters responsible for the peaks in the electronic density of states of $GaAs_{0.5}P_{0.5}$, labeled in Fig. 4(a). The abbreviations $A \equiv$GaP and $B \equiv$GaAs have been used.

Peak	E/t	Major Clusters
1	−2.66	*AAABBA*; *BBBAAA*; *BBAAAABB*; *BAAAABBB*; *BBBAAAAB*
2	−2.58	*ABAABB*; *BBAABA*; *BABAAB*; *BAABAB*; *ABAABABB*; *BBABAABA*
3	−2.46	*AB*; *BA*; *ABBA*; *BAABABAB*; *BABABAAB*
4	−2.42	*ABAB*; *BABA*; *BBABAA*; *AABABB*; *AABBAB*; *BABBAA* *BBABBAAA*; *AAABBABB*; *ABBABBAA*; *AABBABBA*
5	−2.34	*BAAABB*; *BBAAAB*; *BABBAAAB*; *BAAABBAB*; *AABABABB*; *BBABABAA*; *BAABABAB*; *BABABAAB*
6	−2.10	*BAAB*; *ABAABB*; *BBAABA*; *ABBAABAB*; *BABAABBA*
7	−1.74	*BBAA*; *ABABBAAB*; *BAABBABA*
8	−1.44	*ABBBAA*; *AABBBA*; *BAABBBAA*; *AABBBAAB*
9	−1.28	*ABBBABAA*; *AABABBBA*; *AABAABBB*; *BBBAABAA*
10	−1.06	*ABBABA*; *ABABBA*; *AABBAB*; *BABBAA*; *ABABBAAB*; *BAABBABA*; *BABABBAA*; *AABBABAB*
11	−0.98	*ABBBAA*; *AABBBA*; *BAABBBAA*; *AABBBAAB*
12	−0.92	*AAABBB*; *BBBAAA*; *AABBBBAA*
13	1.94	*ABAABB*; *BBAABA*; *ABBBABAA*; *AABABBBA*

band, while the conduction-band spectra only show the sharply peaked fine-structure characteristic of these effects at their high-energy ends. This is due to our choice of sublattice 1 as the disordered one and the choice of the atomic energy of the constitutents of that sublattice as lower than that of the atom on sublattice 2. Interchanging the roles of sublattices 1 and 2 or choosing the atomic energies of the atoms on the disordered sublattice to be higher than that of the ordered one would interchange the role of the clustering effects in the valence and conduction bands.

In the typical persistence alloy spectra, Figs. 1(a) and 2, it can be seen that an impurity band with a sharply structured spectrum begins to form between the conduction and valence bands for small compositions $x \simeq 0.125$. At the same time, the conduction-band spectrum begins to show a sharply peaked structure at the high-energy end. For larger compositions ($x \simeq 0.375$) the impurity-band spectra have broadened and increased in intensity, while still showing sharply peaked structures. At the same time, the valence-band spectrum displays a large number of spectral peaks, while the conduction-band spectrum is still peaked at its high-energy end. For $x = 0.5$, there is no distinction between impurity and valence bands, and the spectra of both consist almost entirely of a large number of sharp peaks. The peaked structure in the spectrum at the top of the conduction band is still there for $x = 0.5$, but it has decreased in intensity and has nearly merged with the rest of the band. For $x > 0.5$ the roles of the impurity and valence bands are interchanged from their roles for $x < 0.5$ with the trends in the spectra with increasing x being essentially the reverse of those just discussed.

The spectra for the typical alloy in the amalgamation limit, Figs. 1(b) and 3, show that, again because of our choice of atomic energies for the disordered sublattice, the majority of the peaked structures occur in the valence-band spectra, although the high-energy end of the conduction-band spectra also display some fine structure. Of course, for all x there is only one valence band and one conduction band, although the valence band appears to almost break up into two to three subbands for some com-

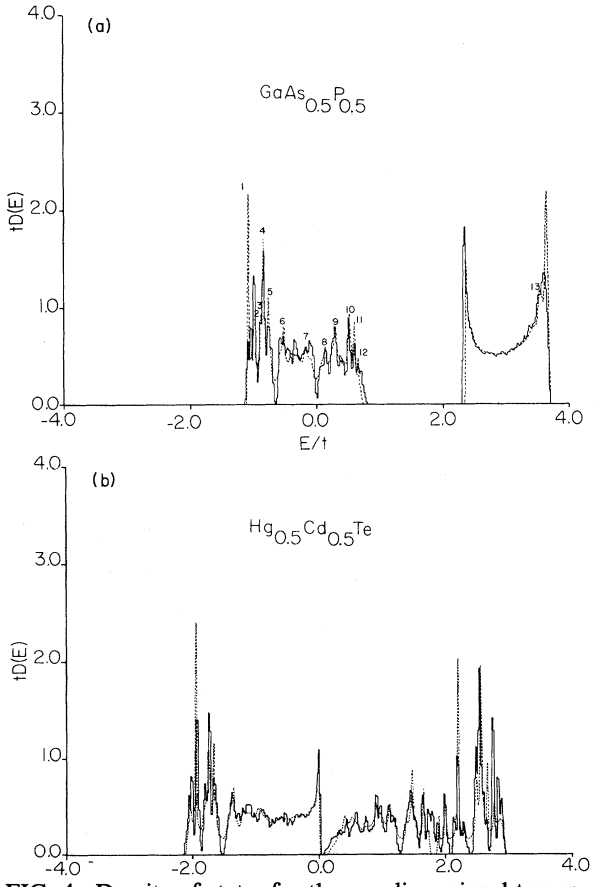

FIG. 4. Density of states for the one-dimensional ternary alloys (a) $GaAs_{0.5}P_{0.5}$ ($\epsilon_C = 2.35t$, $\epsilon_B = 0.80t$, $\epsilon_A = 0.0$) and (b) $Hg_{0.5}Cd_{0.5}Te$ ($\epsilon_C = 0.0$, $\epsilon_B = -0.28t$, $\epsilon_A = 1.59t$) obtained by the embedded-cluster method with a $N_c = 8$ unit-cell cluster (dashed curves) and by the negative-eigenvalue-theorem method for a 10 000-atom random chain (histograms).

positions ($x \simeq 0.5$), and displays a distinct sideband for both small ($x \simeq 0.125$) and large ($x \simeq 0.875$) compositions. For intermediate x, the valence-band spectrum shows a very large number of closely spaced peaks.

C. Dependence on cluster size

To illustrate the effects on embedded-cluster-method calculations of changing the cluster size, we have calculated the density of states using this method for clusters containing $N_c = 2$, 4, 6, and 8 unit cells for a typical alloy in the persistence limit ($\epsilon_C = -\epsilon_B = 2t$, $\epsilon_A = 0.0$, $x = 0.5$). In Figs. 5(a) and 5(b) we display the results of this calculation. The results for the cluster-size dependence of the spectra of an alloy in the amalgamation limit are qualitatively similar to the results for this case.

The results shown in Fig. 5 illustrate how the various peaks originate from the various size clusters. The embedded-cluster method simulates the exact, negative-eigenvalue theorem spectrum very well for $N_c = 8$ [see Fig. 1(a)], reasonably well for $N_c = 6$, and obtains most of the major peaks for $N_c = 4$. From the difference between

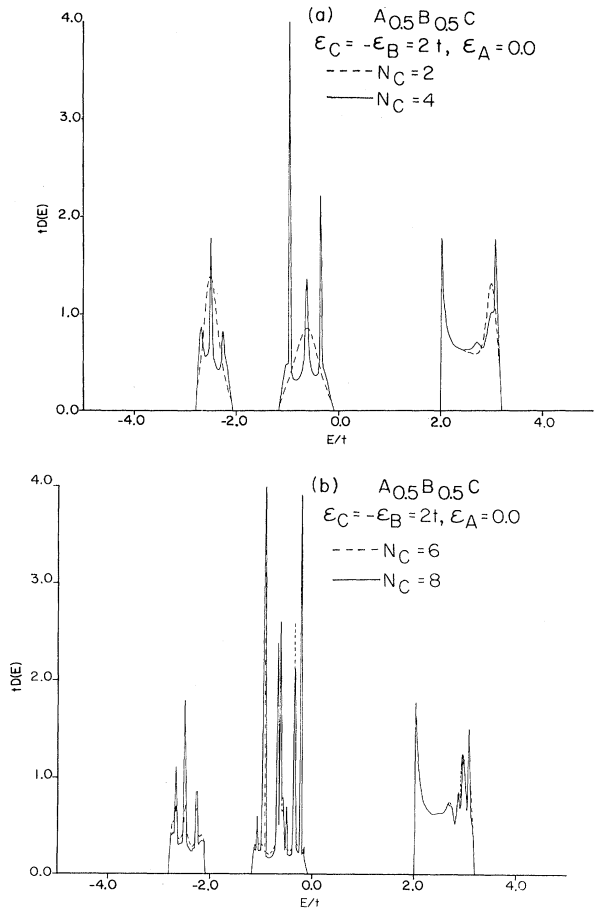

FIG. 5. Dependence of the density of states $D(E)$, obtained by the embedded-cluster method, on the number of unit cells N_c in the cluster for the one-dimensional ternary alloy $A_{0.5}B_{0.5}C$ in the case $\epsilon_C = -\epsilon_B = 2t$, $\epsilon_A = 0.0$. (a) $N_c = 2$ (dashed curve) and $N_c = 4$ (solid curve); (b) $N_c = 6$ (dashed curve) and $N_c = 8$ (solid curve).

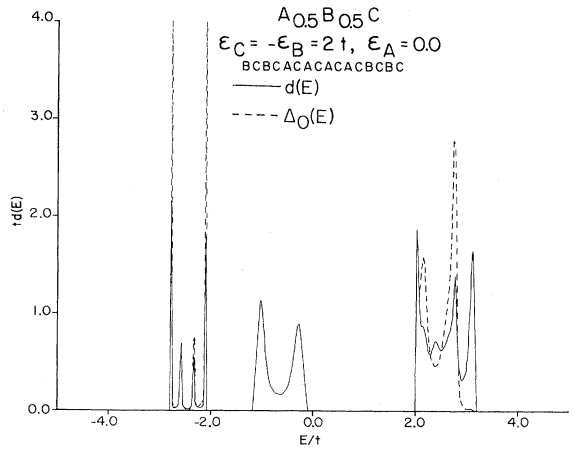

FIG. 6. Global and local central-cell densities of states $d(E)$ (solid curve) and $\Delta_0(E)$ (dashed curve) for a particular cluster configuration obtained by the embedded-cluster method. The cluster size used was $N_c = 8$ unit cells, the configuration chosen for illustration is the one where the alloy constituents are arranged in the form *BCBCACACACACBCBC* and the case illustrated is for the one-dimensional alloy $A_{0.5}B_{0.5}C$ with $\epsilon_C = -\epsilon_B = 2t$, $\epsilon_A = 0.0$.

the $N_c = 6$ and $N_c = 8$ spectra, it is clear that the dependence of the spectra on cluster size is beginning to saturate at $N_c = 8$.

D. Results for single-configuration densities of states

For purposes of illustration, we consider here the global and local densities of states, Eqs. (22a) and (22b), for a single configuration of alloy constituents within the cluster, each of which can also easily be calculated via the embedded-cluster method. It is, on the other hand, difficult to see how to apply the negative-eigenvalue-theorem technique to such a calculation. Figure 6 shows typical results for the global and local densities of states $d(E)$ and $\Delta_0(E)$ for a particular configuration. The results in that figure have been computed for a $N_c = 8$ unit cell cluster for a typical alloy in the persistence ($\epsilon_C = -\epsilon_B = 2t$, $\epsilon_A = 0$, $x = 0.5$) limit. The configuration chosen for display in this figure is the one where the alloy constituents in the cluster are arranged in the form *BCBCACACACACBCBC*. As is also discussed in II, a knowledge of such single-configuration spectra along with the already discussed identification of spectral peaks in the total density of states could be potentially useful information for the analysis of the spectra of nonrandom alloys.

VI. DISCUSSION AND CONCLUSIONS

We have shown that the embedded-cluster method can successfully reproduce the exact numerical electronic densities of states for the one-dimensional ternary alloy $A_xB_{1-x}C$ for all alloy compositions and over a wide range of atomic energy differences of the alloy constituents. Furthermore, it can reproduce these spectra with

relatively small cluster sizes. As may be seen in any of the figures, the spectra obtained for the model alloys considered here are very rich in structure, most of which would be missed in a simple coherent-potential-approximation theory. The fact that the spectra obtained by the use of this method converge for a reasonable cluster size makes the method appear promising for application to the calculation of electronic spectra for real semiconductor alloys. The recent successful use of this method by Gonis *et al.*[17] to treat electronic spectra in real metallic binary alloys further strengthens this potential practicality. In order to successfully apply this theory to realistic models for semiconductor alloys, however, it would be necessary to extend it to include the effects of off-diagonal disorder, which are important for such alloys. The inclusion of such effects into the theory would be straightforward in principle but tedious in practice.[36] It should also be noted that, in contrast with even the "exact" calculations, the embedded-cluster method permits the easy identification of various peaks in the density of states with specific alloy configurations. This is an interesting and useful feature of the method because it has potential applications to the study of nonrandom alloys in which the atoms of one species cluster together.

The principal unsatisfactory features of the spectra calculated by the embedded-cluster method as presented here are essentially the same as those we found for vibrational spectra in I and II have also already been briefly discussed in Sec. V A above. Hence, they will not be discussed in further detail here; the reader is referred to I and II for a detailed discussion.

ACKNOWLEDGMENTS

The authors gratefully acknowledge the support of grants from the National Science Foundation (Grant No. ECS-80-20322) and the Research Corporation, each of which have supported this work at various stages. In addition, we thank J. D. Dow for his many stimulating conversations and his continued encouragement, Tim Henry for helping develop the computer program that generated the spectra via the negative-eigenvalue-theorem method, and Texas Tech University for a grant of computer time to perform these calculations.

APPENDIX A: GREEN'S FUNCTION AND ORTHONORMALIZED EIGENFUNCTIONS FOR THE PERFECT CHAIN

It is not difficult to show that, for the perfect diatomic chain, the real-space matrix elements of the Green's function have the form

$$\langle n,\alpha \mid G^0(E) \mid n',\beta\rangle \equiv G^0_{\alpha\beta}(n,n',E)=\frac{1}{N}\sum_{k,j}\frac{C^j_\alpha(k)[C^j_\beta(k)]^* e^{ik(n-n')a}e^{ika(\alpha-\beta)/2}}{E-E_j(k)}, \tag{A1}$$

where the sum on k is over all wave vectors in the first Brillouin zone, the superscript on the Green's function indicates that it is for the ordered diatomic crystal, j is a band index, $E_j(k)$ is the energy-band function for band j, the $C^j_\alpha(k)$ are the corresponding orthonormalized eigenfunction, and the sum on j goes over all bands.

The energy-band eigenvalues for the diatomic chain are given by Eq. (4) of the text and it is straightforward to find the corresponding orthonormalized eigenfunctions. These have the form

$$C^j_1(k)=\frac{2t\cos(ka/2)}{[(E_j(k)-\epsilon_B)^2+4t^2\cos^2(ka/2)]^{1/2}} \tag{A2}$$

and

$$C^j_2(k)=\frac{[E_j(k)-\epsilon_B]C^j_1(k)}{2t\cos(ka/2)}\ . \tag{A3}$$

By using Eqs. (4), (A2), and (A3) in Eq. (A1), the perfect-chain Green's-function matrix elements can, after much manipulation, be brought into the form given by Eqs. (5a) and (5b), where the function $A(n,n',E)$ in those equations has the form

$$A(n,n',E)=\frac{1}{N}\sum_k\frac{e^{ik(n-n')a}}{[E-E_c(k)][E-E_v(k)]}\ . \tag{A4}$$

Finally, the use of Eq. (4) of the text in Eq. (A4) results, after standard techniques are employed, in the expression for this function given by Eq. (5c).

APPENDIX B: COEFFICIENTS IN THE CUBIC EQUATION

A considerable amount of algebra will reduce the combination of Eqs. (16), (17), and (6) to a cubic equation of the form given in Eq. (18). The coefficients in that equation which result from this manipulation are

$$a_3=2\epsilon_B[\Delta(1-x)(E-\epsilon_C)-\xi^2]\ , \tag{B1}$$

$$a_2=(E-\epsilon_B)(\xi^2-2t^2)+4x\Delta\xi^2 -\Delta^2(1-x^2)(E-\epsilon_C)\ , \tag{B2}$$

$$a_1=\frac{2x\Delta}{\epsilon_B}[2t^2(E-\epsilon_B)-\xi^2(x\Delta+E-\epsilon_B)]\ , \tag{B3}$$

and

$$a_0=\frac{x^2}{\epsilon_B^2}\Delta^2(E-\epsilon_B)(\epsilon^2-2t^2)\ . \tag{B4}$$

In these expressions, the abbreviations

$$\xi^2=(E-\epsilon_B)(E-\epsilon_C)-2t^2 \tag{B5}$$

and

$$\Delta=\epsilon_A-\epsilon_B \tag{B6}$$

have been used.

[1]W. Y. Hsu, J. D. Dow, D. J. Wolford, and B. G. Streetman, Phys. Rev. B **16**, 1597 (1977), and references therein; D. J. Wolford, B. G. Streetman, and J. Thompson, J. Phys. Soc. Jpn. Suppl. A **49**, 232 (1980).

[2]G. B. Stungfellow and H. Kunzel, J. Appl. Phys. **51**, 3254 (1980).

[3]H. J. Lee, L. Y. Juravel, and J. C. Woolley, Phys. Rev. B **21**, 659 (1980).

[4]H. Temken and V. G. Keromidas, J. Appl. Phys. **51**, 3269 (1980).

[5]P. A. Fedders and C. W. Myles, Phys. Rev. B **29**, 802 (1984).

[6]See, for example, D. J. Wolford, W. Y. Hsu, J. D. Dow, and B. G. Streetman, J. Lumin. **18**, 863 (1979).

[7]A. B. Chen and A. Sher, Phys. Rev. B **23**, 5360 (1981); **23**, 5645 (1981); J. Vac. Sci. Technol. **21**, 1381 (1982).

[8]H. Ehrenreich and K. C. Hass, J. Vac. Sci. Technol. **21**, 133 (1982); K. C. Hass, R. J. Lempert, and H. Ehrenreich, Phys. Rev. Lett. **52**, 77 (1984).

[9]S. S. Chan, M. T. Maracyk, and B. G. Streetman, J. Elect. Mater. **10**, 213 (1981).

[10]For a discussion of the theory of alloys, particularly CPA theories, up through 1974, see, for example, R. J. Elliott, J. A. Krumhansl, and P. L. Leath, Rev. Mod. Phys. **46**, 465 (1974), and references therein.

[11]A. Gonis and J. W. Garland, Phys. Rev. B **16**, 2424 (1977).

[12]C. W. Myles and J. D. Dow, Phys. Rev. Lett. **42**, 254 (1979).

[13]C. W. Myles and J. D. Dow, Phys. Rev. B **19**, 4439 (1979).

[14]C. W. Myles, Phys. Rev. B **28**, 4519 (1983).

[15]For a review of this and other numerical attempts at solving the alloy problem, see P. Dean, Rev. Mod. Phys. **44**, 127 (1974), and references therein.

[16]M. J. O'Hara, C. W. Myles, J. D. Dow, and R. D. Painter, J. Phys. Chem. Solids **42**, 1043 (1981).

[17]A. Gonis, W. H. Butler, and G. M. Stocks, Phys. Rev. Lett. **50**, 1482 (1983); A. Gonis, G. Stocks, W. H. Butler, and H. Winter, Phys. Rev. B **29**, 555 (1984).

[18]J. Korringa, Physica (Utrecht) **13**, 392 (1947); W. Kohn and N. Rostoker, Phys. Rev. **94**, 111 (1954).

[19]A persistent spectrum contains features which are characteristic of the quasilocalized nature of the electronic states associated with a single alloy constituent. By contrast, an amalgamated spectrum is hybridized and characteristic of the alloy as a whole, rather than of any component. See, for example, Y. Onodera and Y. Toyozowa, J. Phys. Soc. Jpn. **24**, 341 (1968).

[20]Y. T. Shen and C. W. Myles (unpublished).

[21]For a review of the CPA as applied to electronic spectra in disordered alloys, see H. Ehrenreich and L. Schwartz, in *Solid State Physics,* edited by F. Seitz, D. Turnbull, and H. Ehrenreich (Academic, New York, 1976), Vol. 31.

[22]D. W. Taylor, Solid State Commun. **13**, 117 (1973).

[23]P. Soven, Phys. Rev. **156**, 809 (1967); D. W. Taylor, *ibid.* **156**, 1017 (1967); B. Velický, S. Kirkpatrick, and H. Ehrenreich, *ibid.* **175**, 747 (1968).

[24]P. N. Sen and W. M. Hartmann, Phys. Rev. B **9**, 367 (1974).

[25]An early reference is, for example, F. J. Dyson, Phys. Rev. **92**, 1331 (1953).

[26]The same method will work, in principle, for any translationally invariant effective medium.

[27]In general, for a N_c unit-cell cluster containing $l=xN_c$ AC unit cells and $(1-x)N_c$ BC unit cells, there are $k=\binom{N_c}{l}$ possible configurations. Of course, not all k configurations are physically unique.

[28]For the treatment of impurity spectra in alloys via the embedded-cluster method, we have shown in Ref. 29 that it is necessary to include *all* possible configurations for a given cluster size, even those whose composition differs from the average composition x. In that case, the atypical configurations, whose compositions differ significantly from x, are the ones which make the most important contributions to the wings of the impurity electronic state density. However, in the present case, where the electronic spectra of the alloy itself are being calculated, the neglect of these atypical configurations is a less serious approximation since the intensity of a given peak in the spectrum is proportional to the probability of occurrence of the cluster which produced it. The intensities of the peaks due to the atypical configurations would thus be significantly smaller than those due to the more typical ones. If we were to keep all possible configurations for a N_c unit-cell cluster, the number of required configurations would be $\eta=\sum_{l=0}^{N_c}\binom{N_c}{l}$. See Ref. 29 for further details.

[29]C. W. Myles, J. D. Dow, and O. F. Sankey, Phys. Rev. B **24**, 1137 (1981); C. W. Myles and J. D. Dow, *ibid.* **25**, 3593 (1982).

[30]There are a large number of cluster CPA theories, many of which suffer from nonanalyticity problems, in addition to their computational complexity. One which does not have this problem is given in Ref. 31.

[31]R. Mills and P. Ratanavararaksa, Phys. Rev. B **18**, 5291 (1978); R. Mills, L. J. Gray, and T. Kaplan, *ibid.* **27**, 3252 (1983).

[32]Spectra for other compositions and for parameters corresponding to other "semiconducting alloys" are available from the authors upon written request.

[33]We first assumed that the transfer energy t is equal to 1 eV. The valence-band edge of one or the other of the constituent semiconductors was then arbitrarily chosen to be the zero of energy, thereby fixing the corresponding atomiclike energy (either ϵ_C, ϵ_B, or ϵ_A) at zero. The remaining two atomiclike energies were then determined by fitting the one-dimensional bandgaps of the model at $x=0$ and $x=1$ to the known three-dimensional bandgaps (at $T=OK$) of the two alloy constituents BC and AC. The band gaps we have used are as follows: GaAs, $E_g=1.55$ eV (Ref. 34); GaP, $E_g=2.35$ eV (Ref. 34); CdTe, $E_g=1.59$ eV (Ref. 35), and HgTe, $E_g=-0.28$ eV (Ref. 35) (HgTe is a semimetal).

[34]P. Vogl, H. P. Hjalmarson, and J. D. Dow, J. Phys. Chem. Solids **41**, 364 (1983).

[35]A. Kobayashi, O. F. Sankey, and J. D. Dow, Phys. Rev. B **25**, 6367 (1982).

[36]P. A. Fedders, B. A. Schrauner, and C. W. Myles, Bull. Am. Phys. Soc. **28**, 554 (1983), and unpublished.